GENERAL ELECTRIC

GENERAL ELECTRIC COMPANY
CORPORATE RESEARCH AND DEVELOPMENT
Schenectady, N.Y.

A-C PROPERTIES OF METAL OXIDE VARISTORS

by

L.M. Levinson and H.R. Philipp
Solid State and Electronics Laboratory

Report No. 75CRD175 September 1975

TECHNICAL INFORMATION SERIES

CLASS 1

GENERAL ELECTRIC

General Electric Company
Corporate Research and Development
Schenectady, New York

TECHNICAL INFORMATION SERIES

AUTHOR
Levinson, LM
Philipp, HR

SUBJECT
GE-MOV®

NO. 75CRD175
DATE September 1975

TITLE
A-C Properties of Metal Oxide Varistors

GE CLASS 1
NO. PAGES 7

ORIGINATING COMPONENT
Solid State and Electronics Laboratory
CORPORATE RESEARCH AND DEVELOPMENT SCHENECTADY, N.Y.

SUMMARY

Measurements of the small signal a-c response of ZnO-based ceramic varistors are reported for frequencies f in the range $30 < f < 10^8$ Hz and temperatures T in the range $-200°C < T < 300°C$. The high effective varistor dielectric constant results from the device microstructure with no detectable electrode contribution. The varistor leakage resistance ρ_p drops rapidly with frequency, a crude approximation being $\rho_p \sim 1/\omega$. A broadened relaxation peak in the dissipation factor $D = \tan \delta$ is observed at 3×10^5 Hz at room temperature. The peak has an exponential temperature dependence with an activation energy 0.36 eV.

KEY WORDS
GE-MOV®, a-c properties, dielectric behavior, metal oxide varistors

INFORMATION PREPARED FOR _____

Additional Hard Copies Available From

Corporate Research & Development Distribution
P.O. Box 43 Bldg. 5, Schenectady, N.Y., 12301

Microfiche Copies Available From

Technical Information Exchange
P.O. Box 43 Bldg. 5, Schenectady, N.Y., 12301

A-C PROPERTIES OF METAL OXIDE VARISTORS

L. M. Levinson and H. R. Philipp

I. INTRODUCTION

Metal oxide varistors are a new class of ZnO-based ceramic semiconductor devices with highly nonlinear current voltage characteristics.[1, 2] These devices have current voltage characteristics close to that of back-to-back Zener diodes, but have much greater current and energy handling capabilities.

The varistors are produced by a standard ceramic sintering technique[3] that gives rise to a structure comprised of conductive grains of ZnO surrounded by thin insulating oxide barriers. A schematic microstructure is given in Fig. 1. A typical multicomponent varistor of this type has a composition comprising[3] 97 mole % ZnO, 1 mole % Sb_2O_3 and 1/2 mole % of each of Bi_2O_3, CoO, MnO, and Cr_2O_3.

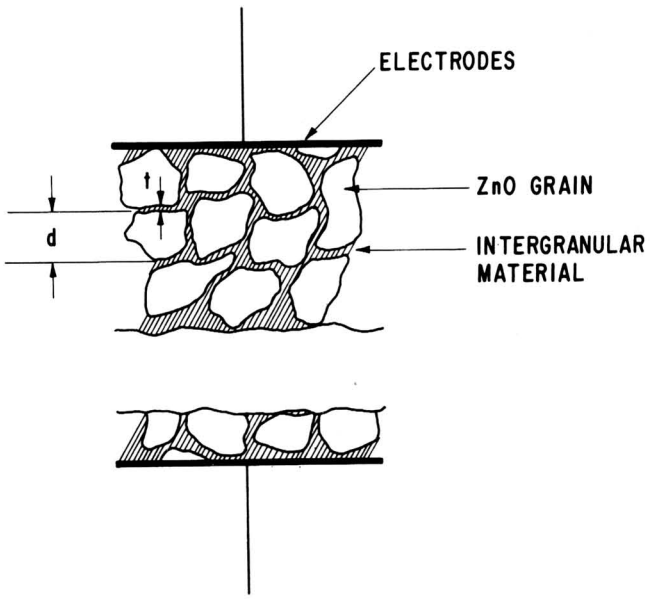

Fig. 1 Schematic depiction of the microstructure of a metal oxide varistor. Grains of conducting ZnO, average size d are completely surrounded by an insulating oxide, thickness t.

In this report we describe measurements of the a-c response of metal oxide varistors. Data have been obtained in the frequency range $30 < f < 10^8$ Hz and for temperatures T in the range $-200°C < T < 300°C$.

We have restricted our attention to a particular metal oxide varistor produced by the General Electric Company [trade name GE-MOV®]. Information as to the composition, microstructure, and phases of this particular ZnO-based ceramic varistor is available elsewhere.[4] We believe that our results are generally applicable to a variety of other multicomponent, highly nonlinear metal oxide varistors (e.g., the composition listed above) and preliminary studies on varistors of differing composition substantiate this viewpoint.

II. RESULTS AND DISCUSSION

The theory of dielectrics is well developed only for linear systems, and is thus inapplicable to a treatment of metal oxide varistors in the breakdown region. If, however, we restrict ourselves to applied voltages much less than the "breakdown voltage," to a first approximation the varistor is ohmic.[2] By keeping this limitation in mind, we may analyze the frequency response and dielectric loss mechanisms in metal oxide varistors using linear response theory.[5-7]

To arrive at an effective equivalent circuit for a metal oxide varistor we shall idealize the ceramic microstructure as shown in Fig. 2. This idealized structure can in turn be represented by the equivalent circuit shown in Fig. 3. Here R_p and C_p are the resistance and capacitance associated with the intergranular layer, respectively. The ZnO grain resistance is denoted r_{ZnO}. The capacitance associated with the ZnO grains is small and will be neglected.

For the purpose of this report we may further simplify the circuit of Fig. 3. In the ohmic or "prebreakdown" region the varistor resistance is high (typically many megohm-cm) and is determined by R_p, the intergranular layer resistance. The ZnO grain resistance is many orders of magnitude lower [$r_{ZnO} \sim 1$ ohm-cm[2]] and is not observable in GE-MOV® varistors for frequencies $f < 10^8$ Hz.[8] Neglecting, r_{ZnO} then, it seems physically plausible to analyze our data in terms of a parallel resistor-capacitor pair, while recognizing that in general the effective capacitor dielectric constant and loss will be frequency dependent.

The equivalent circuit of Fig. 3 assumes that we can neglect electrode effects. To check this we have measured the thickness dependence of the capacitance per unit area of an as-sintered, medium-voltage GE-MOV® varistor.

For a plane-parallel capacitor configuration we have

$$C = C_{el} + \varepsilon \varepsilon_o A/DL \quad , \qquad (1)$$

where C_{el} is the electrode capacitance (if any), and A and L are the capacitor area and electrode spacing, respectively. The intercept at $1/L = 0$, obtained by extrapolating the plot of C vs 1/L, is a measure of C_{el}.

Manuscript received July 22, 1975

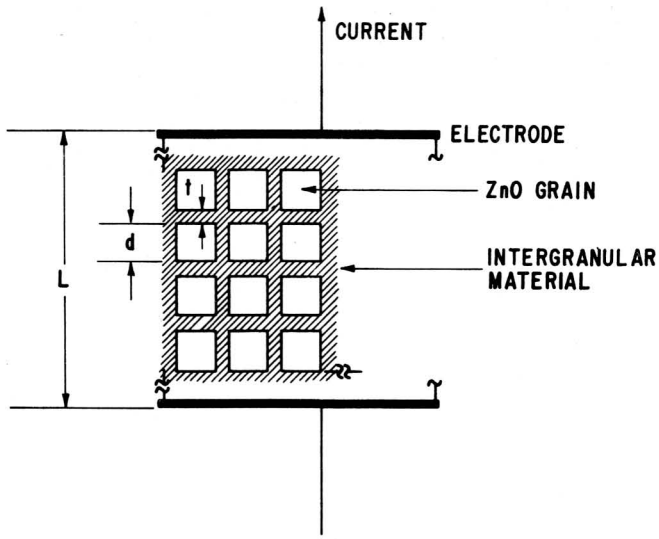

Fig. 2 Idealized microstructure of a metal oxide varistor with grain size d and intergranular barrier t. L is the electrode separation.

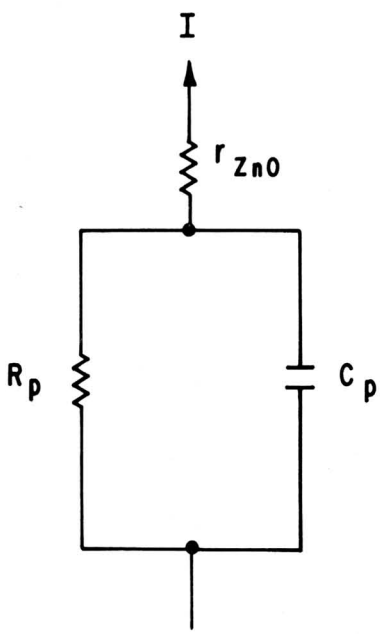

Fig. 3 Simple equivalent circuit representing a metal oxide varistor as a pure capacitance in parallel with a voltage dependent resistor. C_p and R_p are the capacitance and resistance of the intergranular layer, respectively. r_{ZnO} is the resistance of the ZnO grains and is negligible for $f < 10^8$ Hz. For low applied voltages, R_p behaves as an ohmic loss.

Some comments as to the experimental procedure are relevant. The as-sintered varistor was mounted using an air-dry cement and lapped to an appropriate thickness with 1000-mesh SiC grit in a water slurry. Electrodes were In-Ga alloy. The capacitance-thickness measurements were made at 1 kHz.

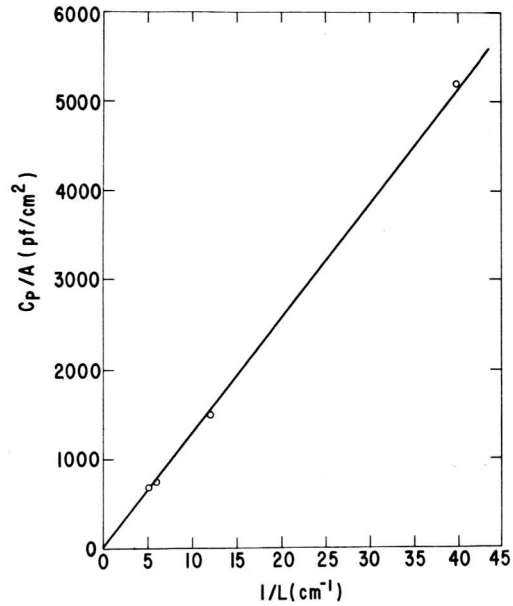

Fig. 4 Variation with inverse thickness of the room-temperature varistor capacitance measured at 1 kHz.

In Fig. 4 we plot C/A vs 1/L and to the accuracy of our results, $C_{el} = O$. Measurement of the dielectric loss D = tan δ showed little variation with L. These results imply that electrode effects are negligible in metal oxide varistors and we have therefore chosen to display our data in intensive units; i.e., we plot dielectric constant ϵ and not capacitance C_p, and resistivity ρ_p and not resistance R_p.

In Figs. 5, 6, and 7 we plot the room-temperature dielectric constant ϵ, dissipation factor D = tan δ and parallel resistivity ρ_p of a GE-MOV® varistor. Data were obtained in the region $30 < f < 10^8$ Hz, and a variety of bridges, Q-meters, and transmission lines were used to cover this frequency range.

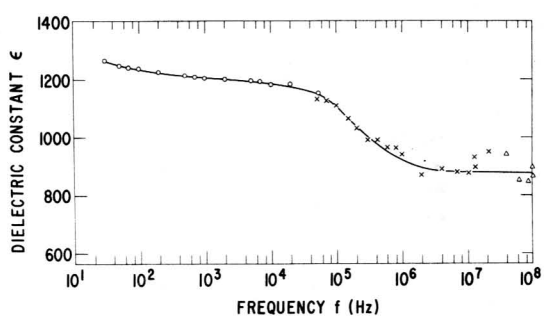

Fig. 5 Variation with frequency of the room-temperature dielectric constant of a GE-MOV® varistor.

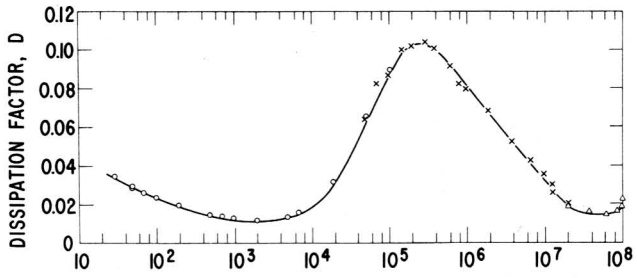

Fig. 6 Dissipation factor D = tan δ vs frequency at room temperature.

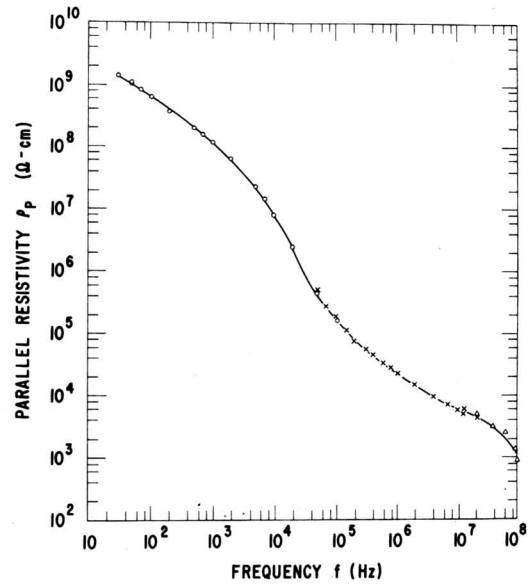

Fig. 7 Parallel resistivity ρ_p of a GE-MOV® varistor at room temperature.

The high dielectric constant evident in Fig. 5 in the audiofrequency range is consistent with previous measurements on metal oxide varistors, (1, 2, 9) and reflects the two-phase nature of these materials. ϵ decreases somewhat from 30 to 10^5 Hz with a sharper dispersive drop evident in the 10^5 to 10^7 Hz range.

In Fig. 6, the dissipation factor D is peaked in the vicinity of 300 kHz. The peak is reminiscent of a typical (broadened) Debye resonance. (6, 7) We note that in the range 30 to 10^8 Hz (6 1/2 orders of magnitude) the dissipation factor varies over a factor of only 10. This has immediate consequences for the frequency dependence of the parallel resistivity, since (6, 7)

$$\rho_p = 1/(\epsilon\epsilon_o \omega D) \quad . \qquad (2)$$

Thus, noting that to a first approximation D and ϵ are roughly constant (see Figs. 5 and 6), we expect $\rho_p \sim 1/\omega$; i.e., the resistivity of GE-MOV® should drop as the inverse frequency.

This behavior is illustrated in Fig. 7 where we plot the parallel resistivity ρ_p vs frequency. Note that ρ_p is about 10^9 Ω-cm at 30 Hz, and $\rho_p \approx 10^3$ Ω-cm at f = 10^8 Hz, implying that the varistor resistivity drops six decades when the frequency increases by 6 1/2 decades. Superimposed upon the general drop in ρ_p with frequency, we observe a dispersive anomaly in the 10^5 - 10^7 Hz region as expected from the results shown in Figs. 5 and 6.

The dispersive dip in ρ_p is absent (10) in the measured frequency range upon cooling to sufficiently low temperatures. In Fig. 8 we give ρ_p for $30 < f < 10^5$ Hz and -196°C < T < 22°C. At T = -196°C (liquid nitrogen) we have $\rho_p \propto 1/f^{0.93}$. At higher temperatures the ρ_p curves of Fig. 8 exhibit a sequence of peaks and troughs superimposed upon the general 1/f variation. These variations are better displayed upon consideration of the frequency dependence of D = tan δ, since from (2) $D \propto \rho_p f$ to a good approximation, and hence the 1/f dependence of ρ_p is factored out. The behavior of D = tan δ is considered in greater detail below.

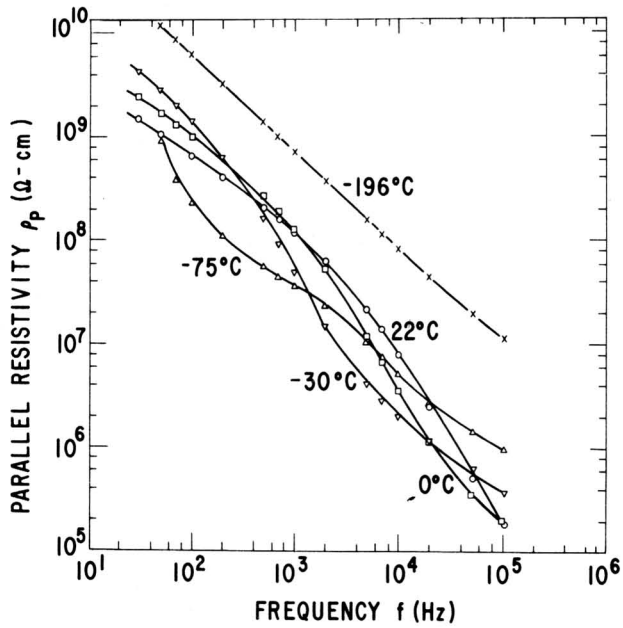

Fig. 8 Temperature and frequency dependence of GE-MOV® parallel resistivity below room temperature.

The frequency dependence of the a-c conductivity of amorphous and glassy materials has been a subject of much recent experimental and theoretical attention. An extremely wide variety (7) of sputtered, anodized, or cast oxides exhibit a frequency dependent conductivity of the type

$$\sigma(\omega) = \sigma_{d\text{-}c} + \sigma_{a.c.}(\omega) \quad , \qquad (3)$$

with the true a-c part of the conductivity having the empirically measured form

$$\sigma_{a\text{-}c} \propto \omega^n \qquad (4)$$

where n is close to unity. The observed behavior is explained in terms of dielectric theory by considering that the disordered specimen is characterized by a wide distribution of relaxation times. In a general sense this corresponds to an extreme broadening of the relatively sharp Debye peak characteristic of systems with a unique relaxation time. For a sufficiently large (and appropriately distributed) range of relaxation times, D = tan δ becomes frequency independent; and from (2), since the capacitance is usually a comparatively weak function of frequency and temperature, we obtain

$$\sigma_p = 1/\rho_p \propto \omega$$

Details of the appropriate choice of relaxation time distributions are given by Smyth.[7]

An alternative (and somewhat equivalent) approach used to derive Eq. (4) considers the detailed motion of charges in dielectric solids. The charges are considered to move from site to site in the solid by discontinuous "hopping" jumps spending, however, most of their time on the sites. The theoretical interpretation of the power law dependence, (4), was first given on this basis by Pollak and Geballe[11] who considered a distribution of hopping probabilities between sites distributed in space and energy in a disordered solid. A variety of references on this topic can be found in the review by Jonscher.[12] This type of behavior is found, for example, in evaporated SiO_x,[13] anodized Al_2O_3[13] and ZrO_2,[14] glassy V_2O_5,[15] and numerous[7, 12] other oxide and non-oxide amorphous dielectrics. It is not unexpected in metal oxide varistors in view of the disordered (Refs. 2, 16) nature of the intergranular barrier layer in these devices.

The high-temperature parallel resistivity shown in Fig. 9 exhibits much the same general features as Fig. 8. ρ_p drops with frequency, but more slowly than at lower temperatures. The 295°C curve has started to flatten out at low frequencies, reflecting the predominance of $\sigma_{d\text{-}c}$ in this temperature-frequency range. At a fixed frequency (e.g., 10^3 Hz) ρ_p drops with temperature.

The temperature dependence of the varistor conductivity is plotted in Fig. 10 where we have chosen to display the data of Figs. 8 and 9 as a function of inverse temperature at fixed frequency. For comparision, the low field d-c conductivity taken from Ref. 2 is also displayed. The data shown here are very similar to the measured temperature dependence of $\sigma_{a\text{-}c}$ in, for example, anodic ZrO_2 and vitreous V_2O_5-P_2O_5 (see Ref. 7, Fig. 18). The Arrhenius plots of Fig. 10 tend toward temperature

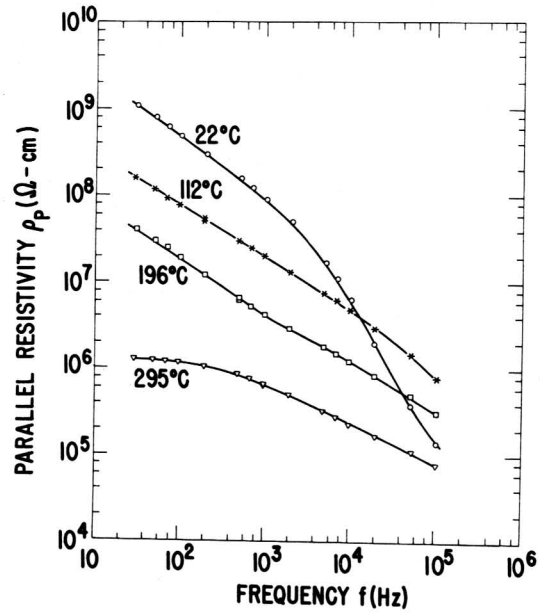

Fig. 9 Temperature and frequency dependence of GE-MOV® parallel resistivity above room temperature.

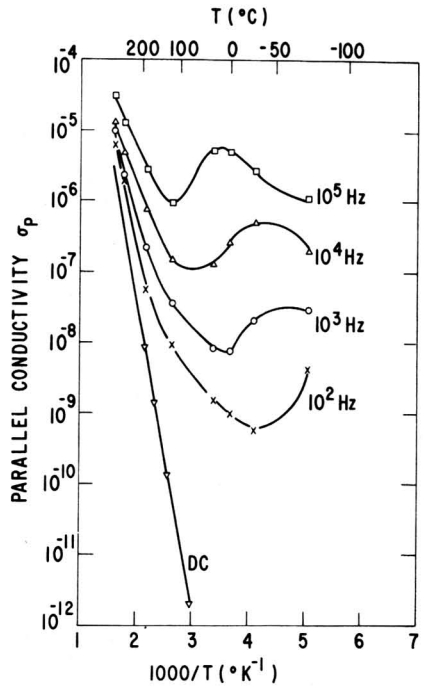

Fig. 10 Arrhenius plot of GE-MOV® varistor conductivity at a variety of fixed frequencies. The d-c data are from Ref. 2.

independence of σ_p at low temperatures and to frequency independence at high temperatures. The apparent activation energy (at higher temperatures) increases with increasing temperature. From the plots

it is clear that at not too high temperatures $\sigma_p >> \sigma_{d-c}$ for $f > 10^2$ Hz; i.e., the a-c part of the conductivity [cf. (3)] dominates in this frequency-temperature region.

In Fig. 11 we plot the dissipation factor D = tan δ as a function of frequency and temperature. It is evident that D exhibits a temperature-dependent broadened Debye-type peak. The peak height increases slightly with increasing T. The peak center is strongly temperature dependent and at room temperature is above 10^5 Hz. The room-temperature variation of the dissipation factor is given in Fig. 6. In Fig. 12 we plot the dissipation factor peak center f_{max} vs inverse temperature. The straight line obtained on the Arrhenius plot indicates that

$$f_{max} = 2 \times 10^{11} e^{-0.36/kT} \text{ Hz} \quad ; \qquad (5)$$

i.e., the peak position is exponentially activated with an activation energy $\varphi = 0.36$ eV. The pre-exponential factor 2×10^{11} is typical of atomic approach frequencies.

It is of interest to ascertain to what extent the loss peaks of Fig. 11 are described by the simple Debye model with a single relaxation time. A standard method[6] to test the applicability of this model is via the so-called Cole-Cole plot. From the Debye equations it can be shown that plot of ε'' against ε' should be a semi-circle in the ε'-ε'' plane at any given temperature. In Figs. 13(a) through (c) we present Cole-Cole plots of ε'' vs ε' at 22°, -30°, and -75°C, respectively. A given point on the curve corresponds to a measurement of real dielectric constant (ε') and loss (ε'') at a particular frequency. The summit of the curve corresponds to that frequency where $\omega\tau = 1$. The lowest and highest frequency points are indicated on each curve.

From Figs. 13(a) through (c) it is evident that the peaks in the dissipation factor curves of Fig. 11 deviate from the pure Debye relaxation behavior, which predicts plots of ε'' vs ε' to lie upon a circle with center on the ε' axis. The experimental data in fact lie on a circular arc centered, as shown, at a point below the ε' axis. The corresponding complex dielectric constant ε^* in such a case can be written[6] as

$$\varepsilon^* - \varepsilon_\infty = (\varepsilon_s - \varepsilon_\infty) \frac{1}{1 + (i\omega\tau)^{1-\alpha}} \quad , \qquad (6)$$

where α corresponds to the angle indicated in Figs. 13(a) through (c) and ε_s and ε_∞ correspond to the static and high-frequency dielectric constants, respectively. When the center of the circle lies upon the ε' axis, i.e., when $\alpha = 0$, Eq. (6) reduces to the familiar Debye equations. A nonzero value of α corresponds to a distribution of relaxation times. A detailed discussion of this point can be found in Refs. 6 and 7. We shall only comment that an α of about 0.2 corresponds to a distribution of

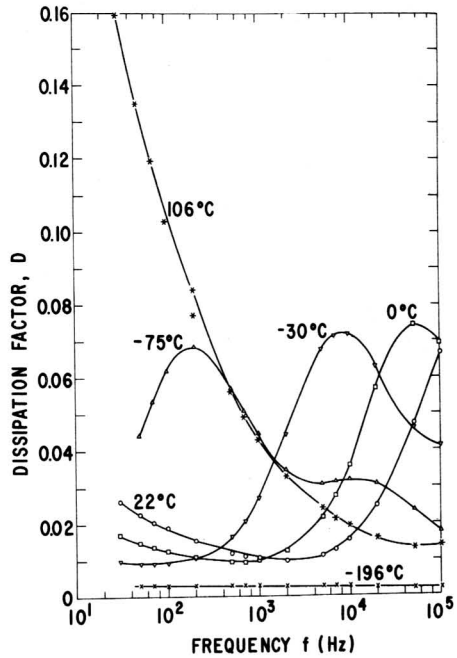

Fig. 11 Dissipation factor D = tan δ vs frequency and temperature. The Debye-like peak is exponentially activated.

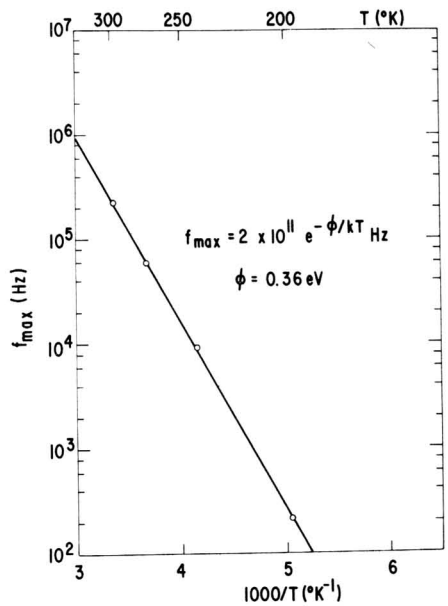

Fig. 12 Arrhenius plot of the frequency f_{max} corresponding to the peak in the dissipation factor.

relaxation times extending over one or two orders of magnitude. We also note that Eq. (6) is by no means implied by the data of Figs. 13(a) through (c). A variety of relaxation time distributions[7] lead to non-circular or flattened Cole-Cole plots of the type obtained for metal oxide varistors.

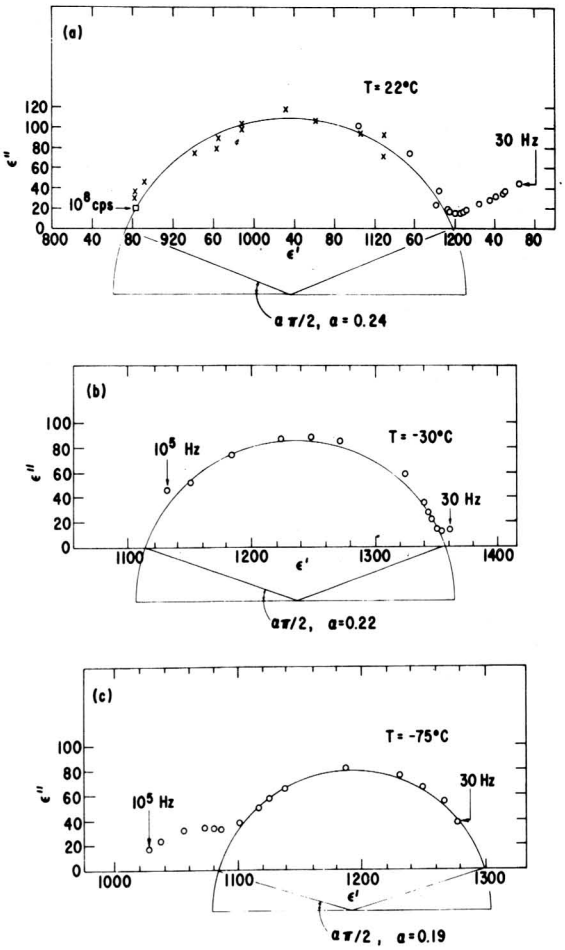

Fig. 13 Cole-Cole plot of ε'' vs ε': (a) T = 22°C; (b) T = -30°C; (c) t = -75°C.

It is tempting to try interpreting the observed (broadened) Debye relaxation peak in terms of the known[1-4] two-phase structure of metal oxide varistors. The Maxwell-Wagner[17] model is routinely used to explain the dielectric behavior of inhomogeneous semiconductors. In particular, the model is often applied to polycrystalline semiconductors assuming layers of high resistivity are present between the grains. A careful examination of the implications of this hypothesis leads one into difficulties, however. For example, the Maxwell-Wagner model predicts[17] that the peak of the dissipation factors occurs at

$$f_{max} \approx \frac{1}{2\pi\varepsilon_0\varepsilon\rho_{ZnO}} \sqrt{\frac{t}{d}} = 5 \times 10^9 \text{ Hz} \quad , \qquad (7)$$

taking[2] $\varepsilon \approx 10$, $t/d \approx 10^3$, $\rho_{ZnO} \approx 1\ \Omega$-cm. This should be compared with the observed value (Fig. 6) which is four orders of magnitude lower at room temperature. In addition, from (7) and Fig. 12 we would conclude that ρ_{ZnO} is exponentially activated. Near room temperature, however, the temperature dependence of the ZnO grain resistance[18] is in fact very slight and this would argue against such an identification. Finally, the Maxwell-Wagner model predicts that at f_{max}, $D \approx \frac{1}{2}\sqrt{d/t} \approx 15$, while the measured values of D at resonance are less than 0.1 (Figs. 6 and 11).

At this point we have not been able to make a positive identification of the origin of the observed Debye relaxation peak. As Smyth[7] has emphasized, the observation of such a phenomenon could arise from (i) an inhomogeneous conductivity distribution (Maxwell-Wagner effect), (ii) an ionic polarization process, or (iii) some type of electronic hopping. On the basis of the discussion above we believe we can rule out explanation (i). An ionic impurity process [hypothesis (ii)] appears unlikely since the same phenomena are observed in varistors that have different compositions. Indeed, recent results[9] on the binary $ZnO\text{-}Bi_2O_3$ system show a dielectric absorption maximum at 10^5 Hz when the material is held at 10°C. This value corresponds exactly to that predicted from Fig. 12. It thus seems unlikely that the resonance observed is associated with either an impurity ion or one of the additive oxides comprising the varistor mix. Nevertheless, at this point we cannot completely rule out an ionic polarization process related to a Zn^{++}, a Bi^{3+} or an O^{-} ion.

A hypothesis consistent with our present data is that the observed broadened Debye resonance is derived from an electronic level either inside the intergranular layer or perhaps at the ZnO-intergranular barrier interface. The latter supposition is made plausible by the observation that the low-field dielectric constant can be affected by the prior application of an a-c high field bias. By symmetry it would appear that an electron in a deep level in the intergranular material bulk would not be affected by a prior a-c stress.

Finally, we wish to emphasize that the general $\rho_p \sim 1/\omega$ behavior of the frequency dependence of the varistor low-field conductivity implies that we are dealing with an essentially disordered intergranular layer. The interface between the intergranular layer and ZnO grain will presumably have surface states or electron traps with widely varying energies. The trap distribution is, however, not completely featureless since this would imply[7] a frequency independent dissipation factor D. The observed Debye-like peak in F (Figs. 6 and 11) must correspond to a preferred energy level in the vicinity of 0.36 eV (Fig. 12). This preferred value is presumably superimposed upon an otherwise uniform energy level distribution.

ACKNOWLEDGMENTS

The help of a number of our colleagues is gratefully acknowledged. G.H. Glover and I.W. Pence facilitated the high-frequency measurements. Helpful discussions were held with M. Garfinkel and E.A. Taft. R.G. Yelle provided competent technical assistance.

REFERENCES AND FOOTNOTES

1. L.M. Levinson and H.R. Philipp, Appl. Phys. Lett. 24, 75 (1974).

2. L.M. Levinson and H.R. Philipp, J. Appl. Phys. 46, 1332 (1975).

3. M. Matsuoka, Jpn. J. Appl. Phys. 10, 736 (1971).

4. J. Wong, J. Appl. Phys. 46, 1653 (1975).

5. H. Frohlich, Theory of Dielectrics, Clarendon Press (1949).

6. V.V. Daniel, Dielectric Relaxation, Academic Press (1967).

7. D.M. Smyth, in Oxides and Oxide Films, Vol. 2, J.W. Diggle ed., Marcel Dekker (1973), p. 95.

8. r_{ZnO} is observable for $f > 10^8$ Hz. L.M. Levinson and H.R. Philipp (unpublished).

9. W.G. Morris, J. Am. Ceram. Soc. 56, 360 (1973).

10. Supplementary measurements have indicated that at liquid nitrogen temperature (-196°C), ρ_p shows no dispersive anomaly down to 0.1 Hz.

11. M. Pollak and T.H. Geballe, Phys. Rev. 122, 1742 (1961).

12. A.K. Jonscher, J. Non-Cryst. Solids 8-10, 293 (1972).

13. F. Argall and A.K. Jonscher, Thin Solid Films 2, 185 (1968).

14. W.S. Chan and C.K. Loh, Thin Solid Films 6, 91 (1970).

15. C.S. Linsley, A.F. Owen, and F.M. Hayatee, J. Non-Cryst. Solids 4, 208 (1970).

16. J. Wong, P. Rao, and E.F. Koch, J. Appl. Phys. 46, 1827 (1975).

17. J. Volger in Progress in Semiconductors, Vol. 4, A.F. Gibson, ed., John wiley, New York (1960).

18. G. Heiland, E. Mollwo, and F. Stockmann, in Solid State Physics, Vol. 8, F. Seitz and D. Turnbull, eds., Academic Press (1969).